Nanoporous Thin Films Based on Polylactide-Grafted Norbornene Copolymers

Sewon Oh,[†] Jin-Kyu Lee,[‡] Patrick Theato,*[,§] and Kookheon Char*[,†]

School of Chemical and Biological Engineering, Center for Functional Polymer Thin Films, Seoul National University, Seoul 151-744, Korea, School of Chemistry, Seoul National University, Seoul 151-747, Korea, and Institute of Organic Chemistry, Johannes Gutenberg-University Mainz, Duesbergweg 10-14, 55099 Mainz, Germany

Received May 24, 2008. Revised Manuscript Received September 20, 2008

Thermally stable vinyl polymerized polynorbornene (PNB) is one of the challenging materials in porous low dielectric films for packaging applications. Nanoporous PNB thin films were obtained with poly(D,L-lactide) (PLA)-grafted norbornene copolymers. Thermally labile PLA chains act as pore generators in PNB films. Thermally stable PNB main chains were synthesized by Pd-catalyzed vinyl polymerization and PLA side chains were grafted onto the PNB main chains by ring opening polymerization. The brittle and poor processible properties of PNB could easily be controlled by the copolymerization with norbornene derivatives. In thin films, the PLA chains were found to thermally decompose at about 250 °C while the PNB matrix was stable during this pore generating process. The porosity of the porous PNB thin films could be controlled up to 18% with pore sizes below 5 nm range by varying the chain length of grafted PLA. Introduction of cross-linking epoxy groups onto the PNB main chains resulted in the formation of well-defined nanopores without any extensive pore collapse during the vitrification of the PNB matrix. Additionally, it is demonstrated that the photopatterning of the thin films could be achieved using photoinitiator.

1. Introduction

High performance polymers, such as polyimides, polyesters, and polynorbornenes, have found a wide range of applications within electronic devices.[1] And also a new organic thermoset polymer, SiLK resin developed by DOW Chemical, was recently developed for faster, smaller, and higher performance integrated circuits.[2−4] Despite their acceptable performance, new packaging materials with improved mechanical properties and lower dielectric constant are still required in order to reduce the time-of-flight and the cross-talk, leading to lowering power supply inductance, capacitance loading, and off-chip driver power.[5] To satisfy these requirements, a promising approach would be the incorporation of nanopores within a polymer matrix.[6−9] Nanopores would reduce the average film dielectric constant because the air gap possesses the lowest dielectric constant with a value of unity. This fact alone explains the considerable interest for porous materials as low dielectric (k) materials.

An established method consists of blending porogens (or pore-generating materials) with organosilicate materials that can then be applied as intermetallic dielectric (IMD) materials.[10−21] The miscibility of two components is the key factor that governs the size and dispersion of pores in the

* To whom correspondence should be addressed. E-mail: theato@uni-mainz.de; khchar@plaza.snu.ac.kr.
[†] School of Chemical and Biological Engineering, Seoul National University.
[‡] School of Chemistry, Seoul National University.
[§] Johannes Gutenberg-University Mainz.

(1) Carter, K. R.; DiPietro, R. A.; Sanchez, M. I.; Swanson, S. A. *Chem. Mater.* **2001**, *13*, 213.
(2) Townsend, P. H.; Martin, S; J; Godschalx, J. P.; Romer, D. R.; Smith, D. W., Jr; Castillo, D.; DeVries, R.; Buske, G.; Rondan, N.; Froelicher, S.; Marshall, J.; Shaffer, E. O.; Im, J.-H. *Mater. Res. Soc. Symp. Proc.* **1997**, *476*, 9.
(3) Martin, S. J.; Godschalx, J. P.; Mills, M. E.; Shaffer, E. O., II; Townsend, P. H. *Adv. Mater.* **2000**, *12*, 1769.
(4) Lin, Q.; Cohen, S. A.; Gignac, L.; Herbst, B.; Klaus, D.; Simonyi, E.; Hedrick, J.; Warlaumont, J.; Lee, H.-J.; Wu, W.-L. *J. Polym. Sci., Part B: Polym. Phys.* **2007**, *45*, 1482.
(5) Rymaszewski, E. J.; Tummala, R. R.; Watari, T. *In Microelectronics Packaging Handbook Part I*; Tummala, R. R., Rymaszewski, E. J., Klopfenstein, A. G., Eds.; Chapman & Hall: New York, 1997; Chapter 1.
(6) Connor, E. F.; Lee, V. Y.; Magbitang, T.; Hawker, C. J.; Volksen, W.; Siemens, R.; DiPietro, R. A.; Hedrick, J. C.; Kim, H.-C.; Miller, R. D.; Hedrick, J. L. *Adv. Mater.* **2004**, *16*, 1525.
(7) Hedrick, J. L.; Carter, K. R.; Richter, R.; Miller, R. D.; Russell, T. P.; Flores, V. *Chem. Mater.* **1998**, *10*, 39.
(8) Carter, K. R.; DiPietro, R. A.; Sanchez, M. I.; Russell, T. P. *Chem. Mater.* **1997**, *9*, 105.
(9) Fu, G.-D.; Yuan, Z.; Kang, E.-T.; Neoh, K.-G.; Lai, D. M.; Huan, A. C. H. *Adv. Funct. Mater.* **2005**, *15*, 315.
(10) Hermans, T. M.; Choi, J.; Lohmeijer, B. G. G.; Dubois, G.; Pratt, R. C.; Kim, H.-C.; Waymouth, R. M.; Hedrick, J. L. *Angew. Chem.* **2006**, *118*, 6800.
(11) Magbitang, T.; Lee, V. Y.; Cha, J. N.; Wang, H.-L.; Chung, W. R.; Miller, R. D.; Dubois, G.; Volksen, W.; Kim, H.-C.; Hedrick, J. L. *Angew. Chem.* **2005**, *117*, 7746.
(12) Magbitang, T.; Lee, V. Y.; Miller, R. D.; Toney, M. F.; Lin, Z.; Briber, R. M.; Kim, H.-C.; Hedrick, J. L. *Adv. Mater.* **2005**, *17*, 1031.
(13) Connor, E. F.; Sundberg, L. K.; Kim, H.-C.; Cornelissen, J. J.; Magbitang, T.; Rice, P. M.; Lee, V. Y.; Hawker, C. J.; Volksen, W.; Hedrick, J. L.; Miller, R. D. *Angew. Chem.* **2003**, *115*, 3915.
(14) Huang, Q. R.; Frank, C. W.; Mecerreyes, D.; Volksen, W.; Miller, R. D. *Chem. Mater.* **2005**, *17*, 1521.
(15) Cha, B. J.; Kim, S.; Char, K.; Lee, J.-K.; Yoon, D. Y.; Rhee, H.-W. *Chem. Mater.* **2006**, *18*, 378.
(16) Lee, H.-J.; Lin, E. K.; Wang, H.; Wu, W.-L.; Chen, W.; Moyer, E. S. *Chem. Mater.* **2002**, *14*, 1845.

10.1021/cm801421w CCC: $40.75
Published on Web 10/29/2008

matrix. However, the main drawback of organosilicate-based materials is their brittleness, particularly for film thickness above 1 μm. To overcome this limitation, thick insulating packaging should be mainly prepared by polymer. As a result, systems based on block copolymers have recently been developed.[1,7−9] For this approach, porogen polymers are polymerized from functional end groups of a thermally stable matrix polymer. The thermodynamic immiscibility of individual blocks on a copolymer chain usually leads to the microphase separation and these microphase separated porogen domains are then removed by physical or chemical means leaving behind air-filled nanoporous structure. Another similar approach is based on the graft copolymerization.[22−25] Over block copolymers, graft copolymers possess the advantage of easier synthesis and usually a wider choice of monomers. Accordingly, porogen polymers are grafted onto the side groups of main chains. Up to now, polyimides have been often chosen as the matrix for insulating nanoporous layers in packaging system, because of its high thermal stability and low dielectric constant. However, this polymer suffers from anisotropic electrical and optical properties, which severely limit the potential applications for electronic devices with small pitch size. Moreover, imidization process is the required step for enhancing the mechanical and thermal stability of the matrix. Amorphous polynorbornene (PNB) is another low dielectric material candidate that could replace polyimides. Norbornene can be polymerized via three different mechanisms, i.e., ring-opening metathesis polymerization (ROMP),[26−31] cationic polymerization,[32] and vinyl polymerization.[33−46] For current applications, vinyl polymerization would be the most interesting mechanism because it leads to polymers with excellent physical properties such as high glass transition temperature, low birefringence, high optical transparency, low water absorption, and low dielectric constant.[47,48] The major drawbacks of norbornene homopolymers are its inherent brittle character and poor solubility in common organic solvents, such as chloroform, tetrahydrofuran or chlorobenzene, thereby limiting its application potentials significantly. Recently, it was shown that these properties can easily be improved through the introduction of a variety of functional groups to the PNB main chains.[47,49] As a consequence, norbornene copolymers, PNB, are now being tested as multichip module (MCM) packaging materials.

In the present study, we report on the novel procedure to generate nanometer-size pores within PNB thin films, with the aim of lowering the dielectric constant. The approach is based on the grafting-from polymerization of thermally labile poly(D,L-lactide) (PLA) side chains by the ring opening mechanism from the thermally stable PNB backbone.[50−52] A microphase separated system with distinct thermal properties was thus generated and converted into porous material after thermal decomposition of the dispersed PLA phase. We demonstrate that varying the chain length of grafted PLA could control pores size as well as pore concentration. Even though the glass transition temperature (T_g) of PNB is high enough, some pores are collapsed in the PNB matrix during the nanopore generation process. To further increase the mechanical resistance of PNB during the nanopore generation process, photo-cross-linkable epoxy functional groups were added to vitrify the matrix prior to thermal decomposition. Furthermore, nanoporous PNB patterns can be generated by the photocross-linking reaction among the epoxy groups through the direct photopatterning method.[53−55] Although nanoporous polymer films based on polyimide have been reported, a systematic study on the synthesis of processible

(17) Nguyen, C. V.; Carter, K. R.; Hawker, C. J.; Hedrick, J. L.; Jaffe, R. L.; Miller, R. D.; Remenar, J. F.; Rhee, H.-W.; Rice, P. M.; Toney, M. F.; Trollsas, M.; Yoon, D. Y. *Chem. Mater.* **1999**, *11*, 3080.
(18) Hyeon-Lee, J.; Lyu, Y. Y.; Lee, M. S.; Hahn, J.-H.; Rhee, J. H.; Mah, S. K.; Yim, J.-H.; Kim, S. Y. *Macromol. Mater. Eng.* **2004**, *289*, 164.
(19) Yim, J.-H.; Seon, J.-B.; Jeong, H.-D.; Pu, L. S.; Baklanov, M. R.; Gidley, D. W. *Adv. Funct. Mater.* **2004**, *14*, 277.
(20) Yang, S.; Mirau, P. A.; Pai, C.-S.; Nalamasu, O.; Reichmanis, E.; Lin, E. K.; Lee, H.-J.; Gidley, D. W.; Sun, J. *Chem. Mater.* **2001**, *13*, 2762.
(21) Long, T. M.; Swager, T. M. *J. Am. Chem. Soc.* **2003**, *125*, 14113.
(22) Chen, Y.; Wang, W.; Yu, W.; Yuan, Z.; Kang, E.-T.; Neoh, K.-G.; Krauter, B.; Greiner, A. *Adv. Funct. Mater.* **2004**, *14*, 471.
(23) Chen, Y.; Chen, L.; Wang, X.; He, X. *Macromol. Chem. Phys.* **2005**, *206*, 2483.
(24) Fu, G. D.; Zong, B. Y.; Kang, E. T.; Neoh, K. G. *Ind. Eng. Chem. Res.* **2004**, *43*, 6723.
(25) Do, J.-S.; Zhu, B.; Han, S. H.; Nah, C.; Lee, M.-H. *Polym. Int.* **2004**, *53*, 1040.
(26) Grubbs, R. H.; Tumas, W. *Science* **1989**, *243*, 907.
(27) South, C. R.; Burd, C.; Weck, M. *Acc. Chem. Res.* **2007**, *40*, 63.
(28) South, C. R.; Leung, K. C.-F.; Lanari, D.; Stoddart, J. F.; Weck, M. *Macromolecules* **2006**, *39*, 3738.
(29) Nair, K. P.; Weck, M. *Macromolecules* **2007**, *40*, 211.
(30) Lee, B. S.; Mahajan, S.; Clapham, B.; Janda, K. D. *J. Org. Chem.* **2004**, *69*, 3319.
(31) Gallagher, M. E.; Enholm, E. *J. Org. Lett.* **2001**, *3*, 3397.
(32) Hino, T.; Endo, T. *Macromolecules* **2003**, *36*, 5902.
(33) Janiak, C.; Lassahn, P. G. *Macromol. Rapid Commun.* **2001**, *22*, 479.
(34) Barnes, D. A.; Benedikt, G. M.; Goodall, B. L.; Huang, S. S.; Kalamarides, H. A.; Lenhard, S.; McIntosh, L. H.; Selvy, K. T.; Shick, R. A.; Rhodes, L. F. *Macromolecules* **2003**, *36*, 2623.
(35) Diamanti, S. J.; Khanna, V.; Hotta, A.; Yamakawa, D.; Shimizu, F.; Kramer, E. J.; Fredrickson, G. H.; Bazan, G. C. *J. Am. Chem. Soc.* **2004**, *126*, 10528.
(36) Sanders, D. P.; Connor, E. F.; Grubbs, R. H. *Macromolecules* **2003**, *36*, 1534.
(37) Mehler, C.; Risse, W. *Macromolecules* **1992**, *25*, 4226.
(38) Kang, M.; Sen, A. *Organometalics* **2004**, *23*, 5396.
(39) Berchtold, B.; Lozan, V.; Lassahn, P.-G.; Janiak, C. *J. Polym. Sci., Part A: Polym. Chem.* **2002**, *40*, 3604.
(40) Li, X.-F.; Li, Y.-S. *J. Polym. Sci., Part A: Polym. Chem.* **2002**, *40*, 2680.
(41) Goretzki, R.; Fink, G. *Macromol. Chem. Phys.* **1999**, *200*, 881.
(42) Wendt, R. A.; Fink, G. *Macromol. Chem. Phys.* **2000**, *201*, 1365.
(43) Wendt, R. A.; Fink, G. *Macromol. Chem. Phys.* **2002**, *203*, 1071.
(44) Puech, L.; Perez, E.; Rico-; Lattes, I.; Bon, M.; Lattes, A.; Moisand, A. *New J. Chem.* **1997**, *21*, 1229.
(45) Lipian, J.; Mimna, R. A.; Fondran, J. C.; Yandulov, D.; Shick, R. A.; Goodall, B. L.; Rhodes, L. F.; Huffman, J. C. *Macromolecules* **2002**, *35*, 8969.
(46) Park, K. H.; Twieg, R. J.; Ravikiran, R.; Rhodes, L. F.; Shick, R. A.; Yankelevich, D.; Knoesen, A. *Macromolecules* **2004**, *37*, 5163.
(47) Grove, N. R.; Kohl, P. A.; Bidstrup Allen, S. A.; Jayaraman, S.; Shich, R. *J. Polym. Sci., Part B: Polym. Phys.* **1999**, *37*, 3003.
(48) Forsyth, J.; Perena, J. M.; Benavente, R.; Perez, E.; Tritto, I.; Boggioni, L.; Brintzinger, H.-H. *Macromol. Chem. Phys.* **2001**, *202*, 614.
(49) Yoo, D. W.; Yang, S.-J.; Lee, J.-K.; Park, J.; Char, K. *Macromol. Res.* **2006**, *14*, 107.
(50) Frick, E. M.; Zalusky, A. S.; Hillmyer, M. A. *Biomacromolecules* **2003**, *4*, 216.
(51) Dobrzynski, P.; Li, S.; Kasperczyk, J.; Bero, M.; Gasc, F.; Vert, M. *Biomacromolecules* **2005**, *6*, 483.
(52) Wang, S.; Lu, L.; Gruetzmacher, J. A.; Currier, B. L.; Yaszemski, M. J. *Macromolecules* **2005**, *38*, 7358.
(53) Chiang, T. H.; Hsieh, T.-E *Int. J. Adhes. Adhes.* **2006**, *26*, 520.
(54) Hogan, Z. L.; Kreller, C. R.; Tran, K. A.; Hart, M. W.; Wallraff, G. M.; Swanson, S. A.; Volksen, W.; Lee, V. Y.; Magbitang, T. P.; Hedrick, J. L.; Hawker, C. J.; Miller, R. D.; Kim, H.-C. *Mater. Sci. Eng., C* **2004**, *24*, 487.
(55) Kim, H.-C.; Wallraff, G.; Kreller, C. R.; Angelos, S.; Lee, V. Y.; Volksen, W.; Miller, R. D. *Nano Lett.* **2004**, *4*, 1169.

PLA-grafted PNB copolymers and the characterization of thermally stable nanoporous PNB thin films has not yet been performed in detail, which is the main objective of the present study.

2. Experimental Section

Materials. All syntheses were performed under a N_2 atmosphere using a standard glovebox and Schlenk techniques. 2,3-Bicyclo[2.2.1]hept-2-ene (or norbornene, NB) **1** was dried over calcium hydride and purified by distillation. 5-Ethoxymethyl bicyclo[2.2.1]hept-2-ene (or 5-ethoxymethyl-2-norbornene, NB-MeOEt) **2** was synthesized from 2,3-bicyclo[2.2.1]hept-5-en-2-yl-methanol (or 5-norbornene-2-methanol, NBMeOH) **3**, as detailed below. 5-Norbornene-2-methanol **3** used as received. 5-Vinyl bicyclo[2.2.1]hept-2-ene (or 5-vinyl-2-norbornene, vinylNB) **5** was used after removing the inhibitor by using column. 3′6-Dimethyl-1,4-dioxane-2,5-dione (or D,L-lactide) was purified through recrystallization from ethyl acetate. m-Chloroperoxybenzoic acid (or mCPBA), sodium hydride, and bromoethane were used as received. Catalysts such as allylpalladium chloride dimmer ($[(\eta^3\text{-allyl})PdCl]_2$) and silver hexafluoroantimonate ($AgSbF_6$) for norbornene polymerization, stannous 2-ethyl-hexanoate ($Sn(Oct)_2$) for lactide polymerization, and triaryl sulfonium hexafluorophosphate salts for photocrosslinking reaction of epoxy groups were used as received. Anhydrous chlorobenzene, anhydrous toluene, anhydrous chloroform, MIBK, and ether were used as reaction solvents. All the reagents were purchased from Aldrich.

Monomer Synthesis. *5-Ethoxymethyl-2-bicyclo[2.2.1]hept-2-ene (**2**).* A 250 mL glass reactor was loaded inside a glovebox with 1.93 g (0.08 mol) of NaH and 100 mL of diethyl ether. The mixture was cooled to 0 °C under stirring, and then 5 g (0.04 mol) of 5-norbornene-2-methanol **3** was added dropwise. After 1 h of reaction, 10.9 g (0.1 mol) of bromoethane was added dropwise. The reaction was continued to stir for 24 h at room temperature. After being washed with deionized water, the organic layer was separated and dried with magnesium sulfate and concentrated by rotary evaporation. The product was purified by column chromatography (SiO_2 with eluant of n-hexane:ethyl acetate (4/1 in v/v)) to yield the product 2 as viscous yellow liquid. Yield: 4.2 g (84%). ^{1}H NMR ($CDCl_3$): δ 6.15−5.90 (m, 2H, CH═CH), 3.8−3.2 (m, 4H, $-CH_2-O-CH_2-$), 3.06−0.82 (m, 7H, norbornene-7H), 1.11 (t, 3H, $-CH_3$).

Copolymerization. *P(NB-r-NBMeOEt-r-NBMeOH) (**4**).* A 250 mL glass reactor was loaded inside a glovebox with 15 g (0.16 mol) of norbornene **1**, 1.347 g (8.86 mmol) of 5-ethoxymethyl-2-norbornene **2**, 1.099 g (8.86 mmol) of 5-norbornene-2-methanol **3**, and 70 mL of dry chlorobenzene. In a separate vial, 0.0653 g (0.177 mmol) of allylpalladium chloride dimer ($[(\eta^3\text{-allyl})PdCl]_2$) and 0.134 g (0.390 mmol) of silver hexafluoroantimonate ($AgSbF_6$) were diluted with 5 mL of dry chlorobenzene and stirred for 20 min. After filtration, this catalyst solution was injected all at once to the monomer mixture. The reaction mixture was stirred for 24 h at room temperature and then poured into HCl containing cold methanol to precipitate the polymer. The precipitated white norbornene copolymer **4** was collected by suction filtration and dried at 90 °C for 24 h under vacuum. We noted that the norbornene copolymer **4** was well-dissolved in organic solvents such as chlorobenzene, toluene, and chloroform. The monomer incorporation ratios, calculated by ^{1}H NMR, were 89, 2, and 9 mol % for NB, NBMeOEt, and NBMeOH, respectively. Yield: 11 g (63%). ^{1}H NMR ($CDCl_3$): δ 3.7−3.25 (br m, 2H, $-CH_2-$ of methanol) and (br m, 4H, $-CH_2-O-CH_2-$ of ethoxymethyl), 3.0−0.7 (br m, 9H, cycloaliphatic of norbornene copolymer), (br s, 1H, −OH), and (br t, 3H$-CH_3$). The weight-average molecular weight (M_w) was determined to be 88 000.

*P(NB-r-vinylNB-r-NBMeOH) (**6**).* The norbornene copolymer **6** was prepared in a similar fashion as the representative example of the norbornene copolymer **4**. A 250 mL glass reactor was loaded inside a glovebox with 7.77 g (0.083 mol) of norbornene **1**, 17.74 g (0.148 mol) of 5-vinyl-2-norbornene **5**, 5 g (0.040 mol) of 5-norbornene-2-methanol **3**, and 70 mL of dry chlorobenzene. In a separate vial, 0.0990 g (0.269 mmol) of allylpalladium chloride dimmer ($[(\eta^3\text{-allyl})PdCl]_2$) and 0.223 g (0.648 mmol) of silver hexafluoroantimonate ($AgSbF_6$) were diluted with 5 mL of dry chlorobenzene and stirred for 20 min. This catalyst solution was injected to the monomer mixture. The reaction mixture was stirred for 24 h at room temperature and then poured into HCl containing cold methanol to precipitate the polymer. The precipitated white norbornene copolymer **6** was collected by suction filtration and dried at 90 °C for 24 h under vacuum. The NB-based copolymer could also be well-dissolved in organic solvents such as chlorobenzene, toluene, and chloroform. The monomer incorporation ratios, calculated by ^{1}H NMR, are 52.5, 35.5, and 12 mol % for NB, vinylNB, and NBMeOH, respectively. Yield: 19.2 g (63%). ^{1}H NMR ($CDCl_3$): δ 5.9−5.7 and δ 5.0−4.8 (br m, 3H, $-CH=CH_2$), 3.8−3.3 (br m, 2H, $-CH_2-$ of methanol), 3.0−0.7 (br m, 9H, cycloaliphatic of norbornene copolymer), and (br s, 1H, −OH). The weight-average molecular weight (M_w) of the copolymer **6** was determined to be 10 000.

Graft Copolymerization. *P(NB-r-NBMeOEt)-g-PLA (**7**).* The graft copolymerization of D,L-lactide from the norbornene copolymer **4** is described here as a representative example. Into a dried 250 mL glass reactor was added 2 g (0.0227 mmol) of norbornene copolymer **4** and 70 mL of anhydrous toluene with a stream of N_2. The mixture was heated to 120 °C for 1 h with stirring, and then 0.5 g (3.472 mmol) of distilled D,L-lactide was added to the mixture. After 10 min, stannous 2-ethyl-hexanoate ($Sn(Oct)_2$) was added to the reaction mixture and refluxed at 120 °C for 24 h. After 24 h, the reaction mixture was poured into cold methanol to precipitate the graft copolymer. This white PLA-grafted norbornene copolymer **7a** was collected by suction filtration and dried at 45 °C for 24 h under a vacuum. Yield: 2.2 g (88%). ^{1}H NMR ($CDCl_3$): δ 5.25−5.15 (br m, 1H, CH of PLA), 4.35 (q, 1H, CH of PLA end group), 3.7−3.3 (br m, 2H, $-CH_2-$ of 5-norbornene-2-methyl), and (br m, 4H, $-CH_2-O-CH_2-$ of ethoxymethyl), 3.0−0.7 (br m, 9H, cycloaliphatic of norbornene copolymer), (br s, 1H, −OH of PLA), and (br t, 3H, $-CH_3$ of ethoxymethyl), 1.45 (br d, 3H, $-CH_3$ of PLA). The PLA-grafted norbornene copolymers were prepared with different PLA contents, varying from 18 to 60 wt %.

The PLA-grafted norbornene copolymer with 30 wt % of PLA **7b**. Two grams (0.0227 mmol) of the norbornene copolymer **4** with 2 g (0.0139 mol) of distilled D,L-lactide. Yield: 3.2 g (80%).

The PLA-grafted norbornene copolymer with 60 wt % of PLA **7c**. Two grams (0.0227 mmol) of the norbornene copolymer **4** with 4 g (0.0278 mol) of distilled D,L-lactide. Yield: 3.2 g (53%).

*P(NB-r-vinylNB)-g-PLA (**8**).* The graft copolymerization of D,L-lactide to the norbornene copolymer **6** was preformed in a similar fashion as outlined above. Into a dried 250 mL glass reactor was added 2 g (0.2 mmol) of the norbornene copolymer **6**, 1 g (6.944 mmol) of distilled D,L-lactide, and 70 mL of anhydrous toluene. This mixture was refluxed at 120 °C for 24 h under N_2 purge. After 24 h, the reaction mixture was poured into cold methanol to precipitate the graft copolymer and this white PLA-grafted norbornene copolymer **8** was collected by suction filtration and dried at 45 °C for 24 h under a vacuum. Yield: 2.68 g (89%). ^{1}H NMR ($CDCl_3$): δ 5.9−5.7 and δ 5.0−4.8 (br m, 3H, $-CH=CH_2$),

Scheme 1. Synthesis of Polylactide-Grafted Norbornene Copolymers

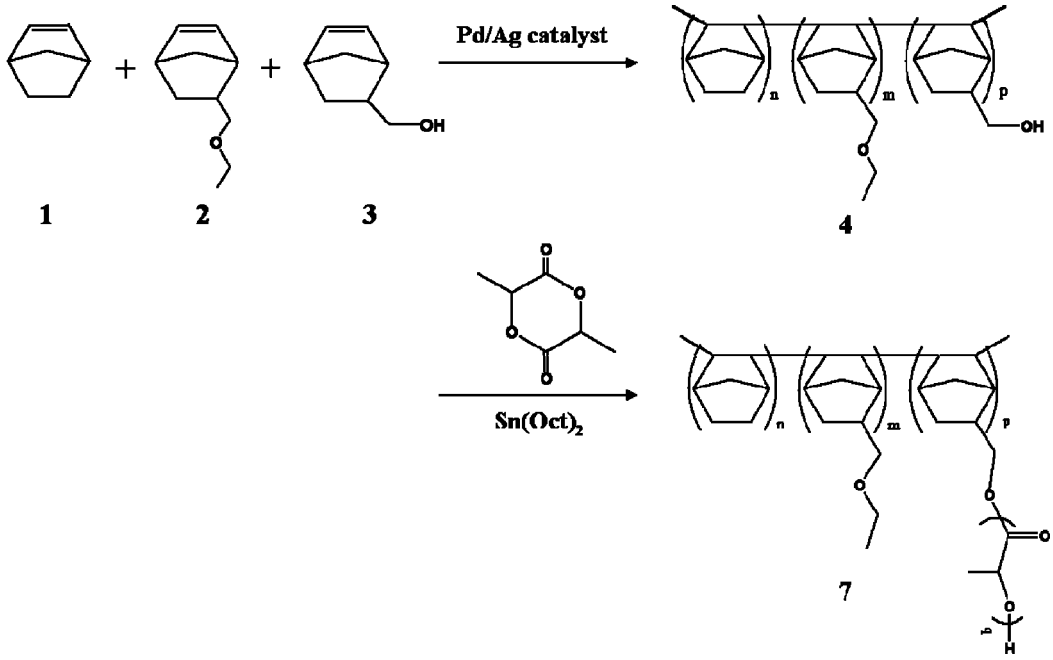

5.25−5.15 (br m, 1H, CH of PLA), 4.35 (q, 1H, CH of PLA end group), 3.7−3.3 (br m, 2H, $-CH_2-$ of 5-norbornene-2-methyl), 3.0−0.7 (br m, 9H, cycloaliphatic of norbornene copolymer), and (br s, 1H, −OH of PLA), 1.45 (br d, 3H, $-CH_3$ of PLA).

Epoxidation of VinylNB. *P(NB-r-epoxyNB)-g-PLA (***9***).* In a 100 mL glass reactor was dissolved 1 g of the graft copolymer **8** containing vinyl side groups in 10 mL of anhydrous chloroform. The mixture was then heated to 50 °C until the graft copolymer **8** was dissolved completely. In a separate vial, 1 g of m-CPBA was dissolved in 10 mL of anhydrous chloroform, and then added to the reaction mixture containing graft copolymer **8** with vigorous stirring for 24 h under N_2 condition.[56−58] After 24 h, the reaction mixture was poured into cold methanol to precipitate the polymer. This white polymer **9** was collected by suction filtration and dried at 45 °C for 24 h under a vacuum. Yield: 0.92 g (92%). ^{1}H NMR ($CDCl_3$): δ 5.25−5.15 (br m, 1H, CH of PLA), 4.35 (q, 1H, CH of PLA end group), 3.7−3.3 (br m, 2H, $-CH_2-$ of 5-norbornene-2-methyl), 3.0−2.7 (br m, 3H, epoxy ring), 3.0−0.7 (br m, 9H, cycloaliphatic of norbornene copolymer), and (br s, 1H, −OH of PLA), 1.45 (br d, 3H, $-CH_3$ of PLA).

Preparation of Nanoporous Thin Films. *P(NB-r-NBMeOEt)-g-PLA Thin Films.* The graft copolymers **7a**, **7b**, and **7c** were dissolved in chlorobenzene at 5 wt % concentration. Thin polymer films with different PLA contents were obtained by spin coating at 2000 rpm for 30 s. These films were annealed at 250 °C for 1 h with a homemade furnace under a N_2 atmosphere to realize nanopores within the PNB thin films. Scheme 1 shows a schematic on the polymerization of graft copolymers **7a**−**c** and Figure 1 represents the nanopore formation of such graft copolymer films.

Preparation of Negatively Patterned Nanoporous Thin Films. *P(NB-r-epoxyNB)-g-PLA Thin Film.* The graft copolymer **9** was dissolved in MIBK at 10 wt % concentration along with 2 mol % of triaryl sulfonium hexafluorophosphate salt as a photoinitiator. Thin polymer films were obtained by spin coating at 2000 rpm for 30 s. The films were subject to exposure to a UV radiation source (wavelength = 254 nm, dose = 554 mJ/cm^2) through a standard photolithographic mask under vacuum. The photoinitiator under the selectively exposed area initiated the cross-linking reaction through the cationic polymerization of epoxy groups. Negative patterns were generated by rinsing with MIBK. The patterned films

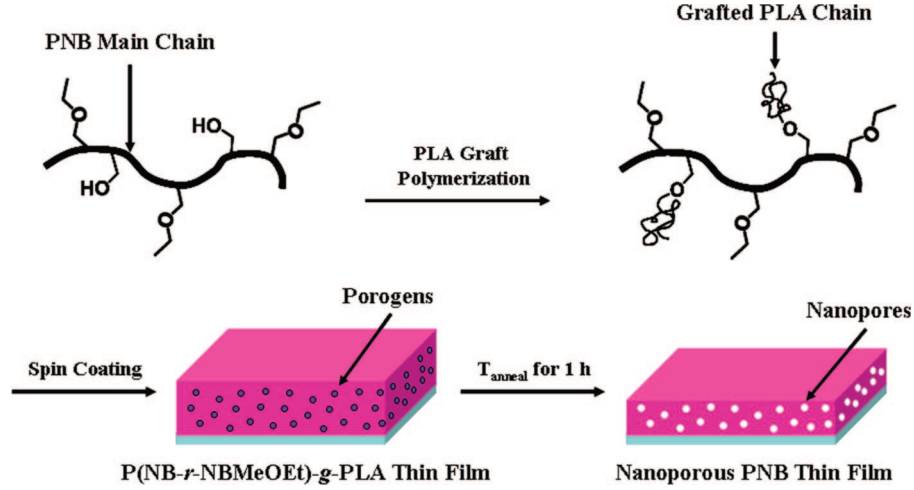

Figure 1. Preparation of nanoporous PNB thin films.

Scheme 2. Synthesis of Polylactide-Grafted Norbornene Copolymers with Photo-Cross-Linkable Epoxy Groups

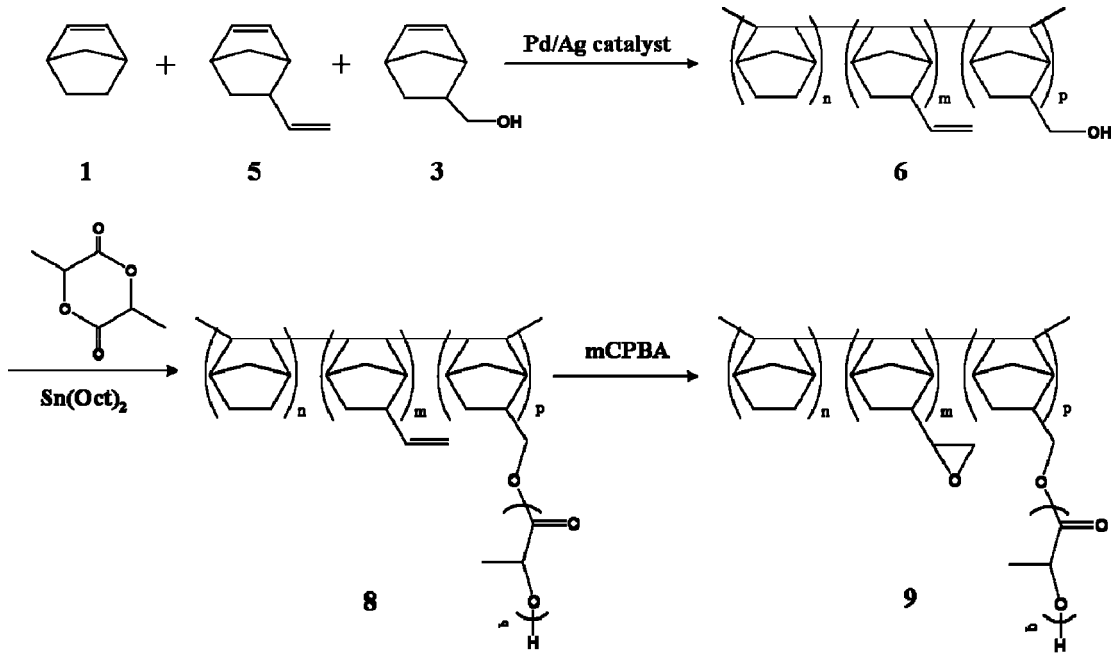

were further annealed at 250 °C for 1 h to generate nanopores within the cross-linked PNB thin film. A schematic on the polymerization of graft copolymer **9** is shown in Scheme 2 and a schematic on the patterning by photo-cross-linking followed by nanopore generation is also shown in Figure 2.

Characterization. ^{1}H NMR spectra were obtained at room temperature using a Bruker, Avance 500 MHz. Gel permeation chromatographic (GPC) analyses were carried out using a Waters Alliance GPC 450 Systems. Chloroform was used as an eluent at a flow rate of 1.0 mL/min and the GPC results were calibrated with respect to polystyrene standards, ranging from 500 to 1 000 000 in molecular weight. Thermal gravimetric analysis (TGA) was performed using a TA model 2050 TGA Instrument under N_2 flow at a heating rate of 10 °C/min from 100 to 700 °C. Fourier transformed infrared spectroscopy (FT-IR) measurements were performed on a JASCO FT/IR 200 spectrometer; 16 accumulations were signal-averaged at a resolution of 4 cm^{-1}. FT-IR spectra were obtained for each film on Si wafers in transmission mode at room temperature. The refractive indices and the thickness of thin films were measured with a variable-angle multiwavelength ellipsometer (Gaertner L2W15S830) with two wavelengths at 633 and 834.5 nm. Cross-sectional morphologies of thin films were observed using a field emission scanning electron microscopy (FE-SEM, JEOL 7401F). Transmission electron microscopy (TEM) was performed on a JEM-2000EXII microscope. The specimens were stained by exposure to ruthenium tetroxide (RuO_4) vapor for 20 min. For TEM measurements, electron transparent films with nominal thickness of 50 ~ 80 nm were microtomed. Synchrotron SAXS measurements were carried out at the 4C2 SAXS beam line at Pohang Light Source (PLS) (λ = 1.54 Å) consisting of Si (111) double crystal monochromators, ion chambers, and a two-dimensional position sensitive detector with 1242 × 1152 pixels. The typical beam size was smaller than 1 × 1 mm^2 and the sample-to-detector distance was 3.1 m. The resulting two-dimensional scattering images were averaged azimuthally to obtain the traces of intensity versus scattering wave vector q ($q = 4\pi\sin(\theta/2)/\lambda$, where λ is the wavelength and 2θ is the scattering angle).

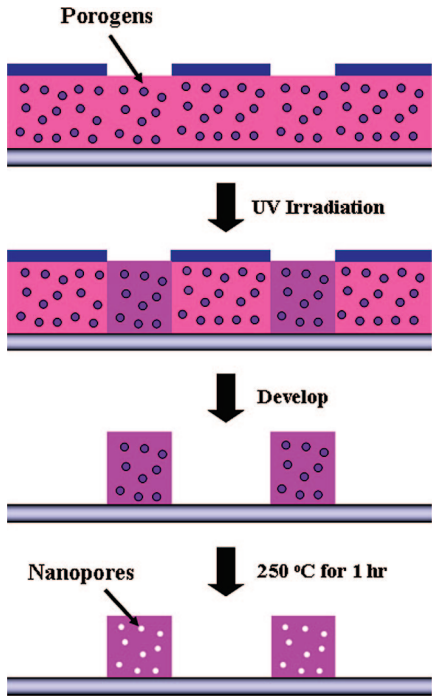

Figure 2. Schematic on the patterning process in the photo-cross-linkable nanoporous PNB system.

3. Results and Discussion

Synthesis of Functionalized Norbornene Monomer and Polymers. Norbornene homopolymers, which have been synthesized through vinyl polymerization, usually do not dissolve in common organic solvents such as chlorobenzene, chloroform, and THF. To increase the solubility of polynorbornene, it is necessary to polymerize functionalized norbornene monomers. As a result, we synthesized the norbornene derivative **2** based on the S_N2 reaction of 5-norbornene-2-methanol with bromoethane, thereby introducing alkyl side chains and flexible ether linkages to the otherwise rigid norbornene backbone. Copolymerization of **2** with norbornene led to the drastic improvement of solubility of the

resulting copolymers, and in turn, to the significant enhancement of processibility into thin films. Two mole percent of **2** is the minimum comonomer content for maintaining reasonable solubility of norbornene copolymers in common organic solvents.

Graft Polymerization. *P(NB-r-NBMeOEt)-g-PLA (**7**).* Scheme 1 illustrates the different steps of synthesis of PLA-grafted norbornene copolymers. First, norbornene terpolymer **4** was synthesized by vinyl copolymerization using allylpalladium chloride dimer ($[(\eta^3\text{-allyl})PdCl]_2$) and silver hexafluoroantimonate ($AgSbF_6$) as catalysts. The ethoxymethyl groups in **2** are intended to provide excellent solubility of the resulting norbornene terpolymer in most common organic solvents, as discussed above. In contrast, norbornene homopolymer and copolymers of norbornene **1** and 5-norbornene-2-methanol **3** with varying composition were not soluble in organic solvents. The molecular weight (M_w) of the norbornene terpolymer **4** was 88 000 with polydispersity index of 1.6. The incorporation ratio of each comonomer in the norbornene terpolymer **4** was determined by ^{1}H NMR and calculated as 89, 2, and 9 mol % for NB, NBMeOEt, and NBMeOH, respectively. As the feed ratio of respective comonomers was 90, 5, and 5 mol %, respectively, the difference between the monomer feed ratio and the incorporation ratio results from the difference in the polymerization reactivity of each monomer. The presence of bulkier ethoxymethyl side groups can also increase the steric hindrance and thus reduce the accessibility to the core metal of the catalyst. The increased coordination of the polar sites of the comonomers 5-ethoxymethyl-2-norbornene **2** and 5-norbornene-2-methanol **3** along with the coordination of olefinic moieties seems to stabilize the intermediate complexes. This resulted in the reduction of activity of catalysts and, in turn, decreased the rate of copolymerization of the three monomers when compared with the homopolymerization of norbornene.

The alcohol functional groups within the terpolymers serve as the initiation sites for the ring-opening polymerization (ROP) of D,L-lactide. Consequently, ROP of D,L-lactide was performed using the terpolymer **4** and stannous 2-ethylhexanoate as a catalyst, yielding the PLA grafted norbornene copolymers **7**. As PLA is polymerized from the hydroxy sites of the norbornene copolymer **4**, this synthetic pathway allows us to control the molecular weight of grafted PLA. The PLA molecular weights were calculated by ^{1}H NMR end functional group analysis. Three different graft copolymers with PLA molecular weights (M_n) of 300, 700, and 1700 have been prepared. The ^{1}H NMR could completely assign the respective groups.[50,52,59−61] The ^{1}H signals of CH groups and methyl groups of the grafted PLA appear at 5.25−5.15 and 1.55−1.45 ppm, respectively. A signal for the CH group at the end unit of PLA appears at 4.35 ppm.

*P(NB-r-epoxyNB)-g-PLA (**9**).* Scheme 2 shows the synthesis of PLA grafted norbornene copolymer containing photocross-linkable epoxy groups. First, norbornene copolymer **6** was prepared by the vinyl polymerization of norbornene, 5-vinyl-2-norbornene, and 5-norbornene-2-methanol. The vinyl group of 5-vinyl-2-norbornene, which will later serve as a post reaction site for the epoxidation, does not participate on the reaction during the vinyl polymerization of norbornene derivatives, as already shown in the literature.[62,63] The molecular weight (M_w) of the norbornene copolymer **6** was 10 000 with a PDI of 2. The incorporation ratio of each monomer, which was again calculated by ^{1}H NMR, was 52.5, 35.5, and 12 mol % for NB, vinylNB, and NBMeOH, whereas the feed ratio were 30, 55, and 15 mol %, respectively. This norbornene copolymer **6** was analyzed by ^{1}H NMR and showed signals for three protons of vinyl groups at 5.9−5.7 and 5.0−4.8 ppm and for three protons from methanol groups at 3.9−3.35 ppm.

The corresponding PLA-grafted norbornene copolymer **8** was obtained by the ring opening polymerization of D,L-lactide based on the copolymer **6** in the presence of $Sn(Oct)_2$ catalyst. The molecular weight (M_w) of the grafted PLA chains was found to be around 300. NMR measurements confirmed that the vinyl side groups remained intact without side reactions during the ring opening polymerization.

In the next step, the epoxidation reaction of the vinyl groups of copolymer **8** was carried out in the presence of mCPBA. This epoxidation step had to be performed after the PLA graft polymerization, because we noted that the epoxy groups were unstable during the PLA polymerization, which was typically carried out at 120 °C. All the vinyl groups could be converted to the epoxy groups, which were again confirmed by ^{1}H NMR. As a result, the copolymer **9** contains the epoxy functional groups as photo-cross-linkable sites, which would result in a vitrified and more thermally stable PNB matrix upon UV treatment.

Thermal Analysis of Graft Copolymers. Amorphous polylactide (PLA) is known to have lower degradation temperature than other pore generating polymers. Accordingly, PLA is a good candidate for thermally generating nanopores within the thin films. Therefore, the thermal behavior of all the PLA-grafted norbornene copolymers (copolymers **7a**−**c**) was evaluated by thermogravimetric analysis (TGA) under N_2 condition in order to determine the weight percentage of PLA and the degradation temperature of each copolymer (see Figure 3). The PLA-grafted norbornene copolymers **7a**−**c** exhibit a two-step degradation process. The temperature range of the decomposition of thermally labile PLA was determined to lie between 170 and 270 °C, whereas the onset decomposition temperature of the norbornene copolymer **4** was found to be at 390 °C. This broad degradation temperature range for PLA is a signature of the random chain scission accompanied by transesterification reactions, as already reported in literature.[64−67] The

(56) Marathe, S.; Sivaram, S. *Macromolecules* **1994**, *27*, 1083.
(57) Kamata, K.; Yonehara, K.; Sumida, Y.; Yamaguchi, K.; Hikichi, S.; Mizuno, N. *Science* **2003**, *300*, 964.
(58) Kim, I. *React. Funct. Polym.* **2001**, *49*, 197.
(59) Cai, Q.; Zhao, Y.; Bei, J.; Xi, F.; Wang, S. *Biomacromolecules* **2003**, *4*, 828.
(60) Schmidt, S. C.; Hillmyer, M. A. *Macromolecules* **1999**, *32*, 4794.
(61) Zalusky, A. S.; Olayo-Valles, R.; Wolf, J. H.; Hillmyer, M. A. *J. Am. Chem. Soc.* **2002**, *124*, 12761.
(62) Zhao, C.-T.; Ribeiro, M. R.; Portela, M. F. *J. Mol. Catal. A* **2002**, *185*, 81.
(63) Lasarov, H.; Pakkanen, T. T. *Macromol. Chem. Phys.* **2000**, *201*, 1780.
(64) Zhao, Y.; Shuai, X.; Chen, C.; Xi, F *Chem. Mater.* **2003**, *15*, 2836.
(65) Boudouris, B. W.; Frisbie, C. D.; Hillmyer, M. A. *Macromolecules* **2008**, *41*, 67.

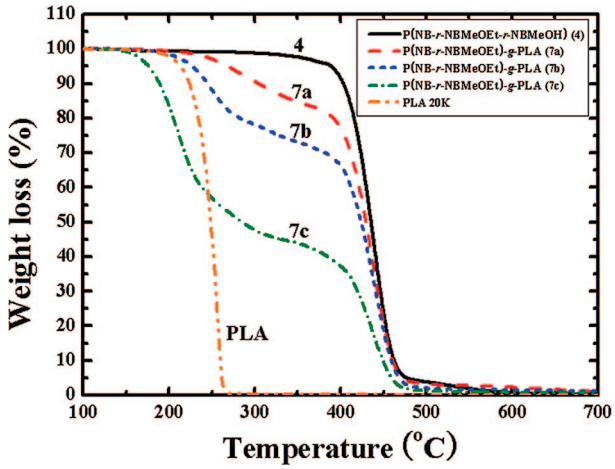

Figure 3. TGA data of norbornene copolymer **4** and PLA grafted norbornene copolymers **7a**−**c** with a heating rate of 10 °C/min under N_2.

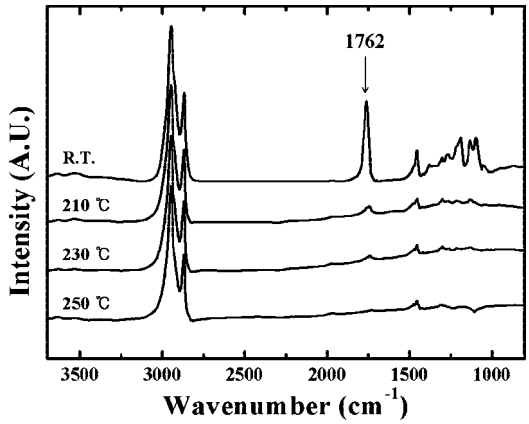

Figure 4. FT-IR spectra showing the structural changes of PLA-grafted norbornene copolymer **7b** thin films at different annealing temperatures.

temperature at which thermal decomposition of labile groups starts to occur is critical for the generation of nanopores within the PNB matrix. It is necessary that the PNB matrix remains thermally stable during the decomposition of PLA in order to prevent the pores from collapse. Comparison of the degradation temperatures of **7a**, **7b**, and **7c** reveals that the degradation temperature decreases with the increase in PLA content or the increase in PLA molecular weight and it appears that short PLA chains grafted onto the norbornene backbone are thermally more stable than the long PLA chains.

Analysis of Structural Change during Anneal Process. Annealing temperature of PLA-grafted PNB films is an important experimental parameter for the optimal generation of pores within the film. In order to accurately establish the PLA degradation temperature, the structural changes of the PLA-grafted norbornene copolymer **7b** film were monitored by IR experiments at different annealing temperatures. Figure 4 shows the FT-IR spectra obtained after annealing the films under N_2 atmosphere for 1 h at 210, 230, and 250 °C, respectively. The strong peak intensities at around 1762 and 1240 cm^{-1} are assigned to the C═O stretching and the C−O stretching of the PLA ester groups, respectively. Intense peaks at around 2700−3200 cm^{-1} are assigned to the sp^2 CH stretching peaks from the PNB main chains. As the annealing temperature is increased, the ester stretching peak intensities originating from PLA decrease and eventually disappear almost completely at 250 °C, indicating the full degradation of PLA. In contrast, the sp^2 CH stretching peak intensities originating from the PNB main chains does not change within this temperature range, demonstrating that the PNB main chains are stable during the degradation process of PLA. As a consequence, the annealing temperature for the PLA degradation was chosen at 250 °C.

Image Analysis of Nanoporous PNB Thin Films. In order to obtain detailed information on the internal structure of the norbornene copolymer **4** as well as the PLA-grafted norbornene copolymer **7b** films, TEM images have been taken (see the Supporting Information, Figures S1a and S1b, respectively). The domain size and distribution of the grafted PLA chains within the PNB matrix have been identified after the films were stained with RuO_4, which reacts preferably with the C═O groups of PLA. Black spots are clearly visible in the TEM image of PLA-grafted norbornene copolymer **7b** film, indicating the dispersion of grafted PLA domains within the PNB matrix. It is also noted that the randomly distributed PLA domains have diameters below 5 nm.

Films of PLA-grafted PNB before and after the anneal temperature to generate pores within the films have been examined by FE-SEM and the results are summarized in Figure 5. All the PLA-grafted norbornene copolymer **7a**−**c** films were prepared by spin casting followed by annealing at 250 °C for 1 h under N_2 purge. The cross-sections of the thin films show that nanoporous PNB thin films were much rougher and textured after the annealing process. The large difference in electron density between pores and the matrix within the resolution of FE-SEM implies the formation of nanoporous structures within the films (see images b, d, and f in Figure 5). In general, it is noted that the roughness and texture of the cross-sections of nanoporous PNB thin films increase as the PLA concentration is increased. Furthermore, the increase in the pore size is also predicted with the increase in the molecular weight of PLA chains. Even though the PNB matrix is thermally stable at the annealing temperature established earlier, the decrease in the overall film thickness was observed, indicating that pores generated by the decomposition of PLA chains have been further collapsed during the annealing process. As the PLA graft chain length is increased, the change in film thickness before and after the thermal treatment also increases (see the Supporting Information, Figure S2). The change in film thickness before and after the thermal treatment correlates very well with the pore collapse in PNB films during thermal treatment. The glass transition temperature (T_g) of PLA-grafted PNB copolymers is the main factor leading to pore collapse. To check T_g values of norbornene copolymer **4** and PLA grafted norbornene copolymers **7a**−**c**, we conducted the DSC experiments up to 230 °C under N_2 (see the Supporting Information, Figure S3). From the DSC data, we were able to locate the T_g of PLA-grafted copolymer **7c** as 45 °C. This

(66) Sivalingam, G.; Vijayalakshmi, S. P.; Madras, G. *Ind. Eng. Chem. Res.* **2004**, *43*, 7702.
(67) Sivalingam, G.; Karthik, R.; Madras, G. *J. Anal. Appl. Pyrolysis* **2003**, *70*, 631.

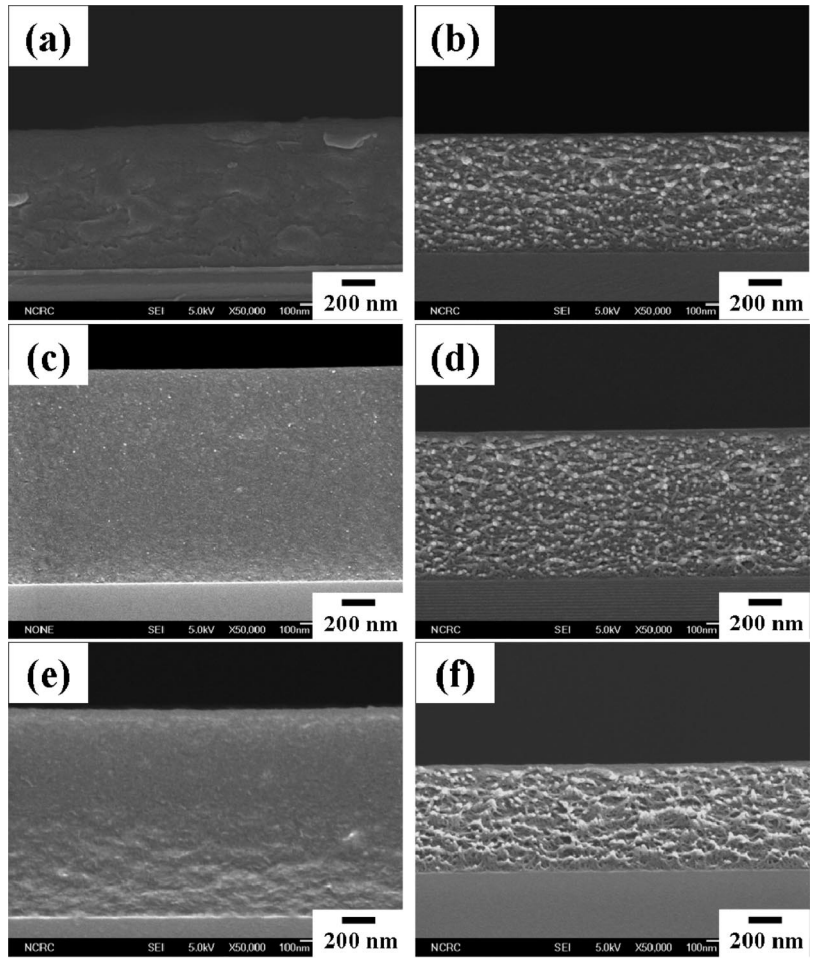

Figure 5. Cross-sectional FE-SEM images of (a) PLA-grafted norbornene copolymer **7a** thin film and (b) annealed film at 250 °C for 1 h under N_2; (c) **7b** thin film and (d) annealed film at 250 °C; (e) **7c** thin film and (f) annealed film at 250 °C.

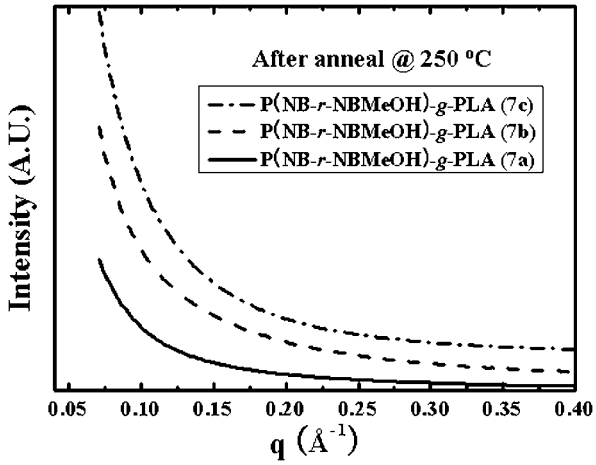

Figure 6. Small-angle X-ray scattering (SAXS) profiles of PLA-grafted norbornene copolymers **7a**−**c** after annealing at 250 °C for 1 h under N_2.

transition temperature indicates the T_g of long PLA side chains. In contrast, we cannot locate T_g values of other copolymers (**7a** and **7b**) with relatively short PLA side chains. This result indicates that thermally stable PNB chains could maintain the thermal stability of PLA-grafted norbornene copolymers to some extent when the length of PLA side chains is short. However, we observed from the measurement of film thickness before and after thermal treatment that nanopores formed are collapsed during the thermal treatment. Although T_g of the copolymers is higher than the thermal treatment temperature, it is likely that the films become softened near the T_g, leading to pore collapse to some degree during the thermal treatment process.

Mechanical Properties of Nanoporous PNB Thin Films. Mechanical properties of nanoporous PNB thin films were measured with nanoindenter in dynamic contact mode (DCM) (see the Supporting Information, Figure S4). Because all the reported values were read at 50 nm of the displacement depth, which is about one-tenth of the total film thickness, the substrate effect could be safely neglected. As the porosity is increased, both modulus and hardness of the nanoporous films decrease. The elastic modulus and surface hardness still maintain values at 4.66 and 0.26 GPa, respectively, even though porosity of the nanoporous films is increased up to 18%. The prepared nanoporous thin films thus have mechanical properties relevant for applications in packaging system.

Small-Angle X-ray Scattering Analysis of Nanoporous PNB Thin Films. To follow the nanopore formation during the thermal anneal process, small-angle X-ray scattering (SAXS) experiments have been performed on the parent norbornene copolymer **4** as well as on the PLA-grafted norbornene copolymers **7a**−**c** after nanopore generation, which was described above. The scattering profiles obtained

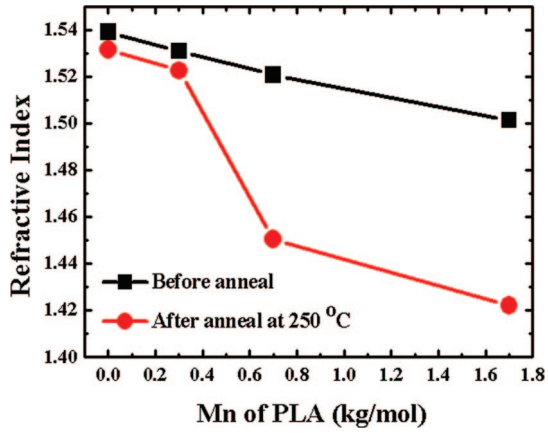

Figure 7. Changes in refractive index of norbornene copolymer **4** and PLA-grafted norbornene copolymers **7a**−**c** thin films, before and after annealing at 250 °C for 1 h under N_2 plotted against PLA molecular weight.

from those samples are shown in Figure 6. The scattering intensity from the norbornene copolymer films is plotted against the scattering vector $q = (2\pi/\lambda)\sin\theta$, where λ is the wavelength (1.54 Å) and 2θ is the scattering angle. For all the films tested, the SAXS profiles show the monotonic decrease in scattering intensity as q is increased, indicating that the nanopores generated after the anneal process are randomly dispersed within the PNB matrix and the pore size is not monodisperse.[1,7,8,17] We believe that there is no appreciable ordered microphase separation in this graft copolymer system and the grafted PLA chains are simply trapped and degraded in highly nonequilibrium state. Using the Debye−Bueche analysis, we can determin the correlation length that would yield the average domain size.[68,69] According to the Debye−Bueche theory for porous materials, the scattering intensity near $q \approx 0$ is given by

$$I(q) = \frac{I_0}{(1+\xi^2 q^2)^2}$$

where I_0 is the zero-angle scattering intensity and ξ is the correlation length describing the average size of heterogeneities in the system. The two physical quantities, ξ and I_0, are thus determined from the slope and the intercept of the plots (see the Supporting Information, Figure S5). The pore volume fraction, which is equal to the porosity, was estimated from the measurements of refractive indices (see Figure 7). An average pore size of approximately 15 Å was obtained for all the samples.

Refractive Index Traces of Nanoporous PNB Thin Films. The refractive index of a thin film is governed by the film density, which is controlled by the film composition. Introducing pores within a thin film changes the film composition as well as film density and thereby controls the refractive index. The refractive indices of PLA-grafted norbornene copolymer **7a**−**c** films have been measured after annealing at 250 °C for 1 h under N_2 purge. With the increase in PLA content in the PNB thin films, the refractive index decreases from 1.53 to 1.42 after thermal treatment (see Figure 7). The porosity of nanoporous PNB films can be estimated from the Lorenz−Lorentz equation[70]

$$\frac{n_c^2 - 1}{n_c^2 + 2} = (1 - P)\frac{n_0^2 - 1}{n_0^2 + 2}$$

with n_c the refractive index of the nanoporous film, n_0 the refractive index of PNB film without porogens, and P the porosity. For a nanoporous PNB film with a refractive index of 1.42, a porosity of 18% could be estimated. The dielectric constant (k) also decreases from 2.70 to 2.30 after thermal treatment, with the increase in the PLA content of PNB thin films (see the Supporting Information, Figure S6). These changes are in good agreement with the changes of refractive indices. Using the norbornene copolymers **7a**−**c**, we could control the porosity of nanoporous PNB films up to 18% without further matrix vitrification. However, as the chain length of PLA is increased, the thermal stability of the PNB matrix decreases such that some pores collapse during the thermal treatment. In order to avoid the further collapse of nanopores within the PNB matrix, increased thermal and mechanical stability of the PNB matrix is crucial, which led us to introduce cross-linking moieties into the PNB matrix.

Table 1. Characteristics of PLA-Grafted Norbornene Copolymers

sample	norbornene copolymer derived form	NBMeOH (mol %)[a]	PLA Mn ($\times 10^3$)[a]	PLA composition (wt %)[b]	porosity (%)[c]
7a	P(NB-*r*-NBMeOEt-*r*-NBMeOH) **4**	9	0.3	18	2
7b	P(NB-*r*-NBMeOEt-*r*-NBMeOH) **4**	9	0.7	30	14
7c	P(NB-*r*-NBMeOEt-*r*-NBMeOH) **4**	9	1.7	60	18
8	P(NB-*r*-vinylNB-*r*-NBMeOH) **6**	12	0.3	23	
9	P(NB-*r*-epoxyNB-*r*-NBMeOH)	12	0.3	23	20

[a] Calculated from ^{1}H NMR spectra. [b] Estimated from thermogravimetric analysis. [c] Calculated from refractive indices based on the Lorenz−Lorentz equation.

Photo-Cross-Linkable and Photopatternable Nanoporous PNB System. As the thermal stability of norbornene copolymers **7a**−**c** is not sufficient to prevent the pore collapse during the thermal annealing process, the introduction of cross-linkable epoxy functional groups into the polynorbornene was assumed to enhance the matrix stability. Using a photo initiator, triaryl sulfonium hexafluorophosphate, photoinitiated cationic polymerization of epoxy groups grafted to the PNB backbone not only result in the cross-linking reaction among epoxy groups to enhance mechanical and thermal stability, but also provide the possibility to photopattern the thin films. Additionally, the photo-cross-linking process guarantees that the matrix can be cross-linked at temperature below the pore generating temperature.

Thin films of the PLA-grafted norbornene copolymer **9** were again prepared by spin coating. The thin films were then exposed to a deep UV radiation source through a standard photolithographic mask. Thereby, the cross-linking reaction of epoxy groups grafted onto PNB was initiated only

(68) Debye, P.; Bueche, A. M. *J. Appl. Phys.* **1940**, *20*, 518.
(69) Iiyama, T.; Kobayashi, Y.; Kaneko, K.; Ozeki, S. *Colloids Surf., A* **2004**, *241*, 207.
(70) Yoon, D. Y.; Ro, H. W.; Park, E. S.; Lee, J.-K.; Kim, H.-J.; Char, K.; Rhee, H.-W.; Kwon, D.; Gidly, D. W. *Mater. Res. Soc. Symp. Proc.* **2003**, *766*, E6.5 E 6.5.

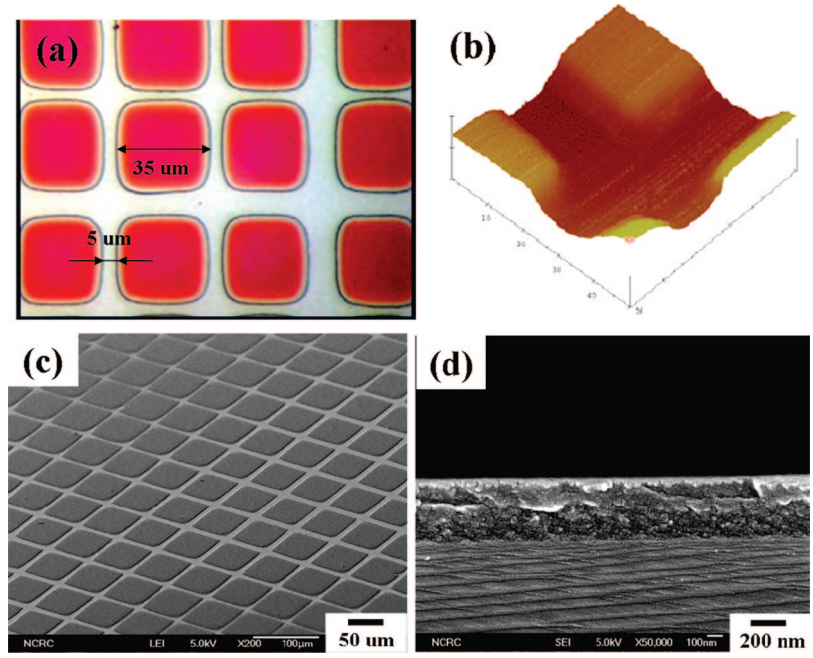

Figure 8. (a) Optical micrograph; (b) AFM image; (c) FE-SEM image (top-view); (d) cross-sectional FE-SEM image of a negatively patterned nanoporous PNB thin film.

within the selectively exposed area.[53,71] Afterward, the negative patterns were developed by rinsing with MIBK, followed by annealing at 250 °C under a N_2 atmosphere to generate porous structure within the film by decomposition of the grafted PLA chains. Structural changes within the film during the photo-cross-linking and the thermal annealing step were again monitored by FT-IR (see the Supporting Information, Figure S7).

Figure 8 shows the images of negatively patterned nanoporous PNB thin films obtained with by optical microscopy, AFM, and FE-SEM. Well-defined patterns are obtained by the direct patterning method. The feature size of the patterns is 35 μm and the line width is 5 μm. Figure 8d shows the cross-sectional FE-SEM images of a patterned nanoporous PNB thin film after thermal annealing, revealing the textured cross-sections as an evidence of pore generation. For detailed investigation of cross-linked nanoporous PNB structure, thick photo-cross-linkable PNB films were prepared and the cross-sectional structure was analyzed by FE-SEM. For this purpose, a PLA-grafted norbornene copolymer **9** film with PLA composition of 23 wt % was spin-casted, irradiated under 254 nm UV light, and annealed at 250 °C for 1 h under N_2 purge. The cross-sectional texture of the nanoporous PNB thin film after annealing is much rougher than that before the annealing process. Nanopores with a diameter below 5 nm could be seen inside the PNB matrix, as shown in Figure 9. Additionally, we noted that the refractive index decreases during the pore generating process from 1.48 to 1.36. From the Lorenz-Lorentz equation, the porosity of this nanoporous film was estimated to be 20%. It is thus concluded that most of nanopores generated during the degradation of PLA chains do not collapse extensively in this thermally stable and photo-cross-linkable PNB matrix.

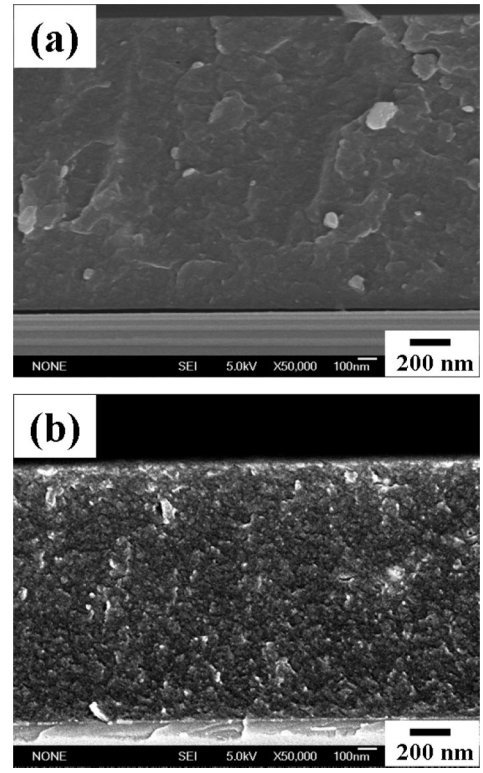

Figure 9. Cross-sectional FE-SEM images of (a) PLA-grafted norbornene copolymers **9** thin film and (b) annealed film at 250 °C for 1 h under N_2.

4. Conclusion

In this contribution, we described the synthesis of PLA-grafted norbornene copolymers and the preparation of nanoporous polymer thin films thereof. Nanoporous thin films were realized by the decomposition of PLA as porogens in thermally stable PNB matrices. We rationally prepared norbornene derivatives and copolymerized these monomers to yield processible and thermally stable norbornene copoly-

(71) Cavalli, G.; Banu, S.; Ranasinghe, R. T.; Broder, G. R.; Martins, H. F. P.; Neylon, C.; Morgan, H.; Bradley, M.; Roach, P. L. *J. Comb. Chem.* **2007**, *9*, 462.

mers. It was found that the porosity of porous PNB thin films could be controlled up to 18% by varying the chain length of grafted PLA. Although the norbornene copolymer is thermally stable, partial collapse of nanopores within the film was also observed. However, the introduction of cross-linkable epoxy moieties into the PNB copolymer prevented the extensive pore collapse. Additionally, it was possible to photopattern these PNB films. The work presented here could present a new class of polynorbornene copolymers, which are readily processible and can yield nanoporous polymer thin films by simple synthetic pathways described in this study. These may find good use in packaging applications based on the thermal stability of PNB.

Acknowledgment. This work was financially supported by the Korea Science and Engineering Foundation (KOSEF) grant through the Acceleration Research (R17-2007-059-01000-0) and the NANO Systems Institute-National Core Research Center (R15-2003-032-02002-0) funded by the Korea Ministry of Education, Science and Technology (MEST). We also acknowledge the financial support from the Korean Ministry of Education, Science and Technology through the Brain Korea 21 Program at Seoul National University and the International Research Training Group (IRTG) (2006-IRTG-001) Mainz-Seoul Program jointly funded by the KOSEF of Korea and the Deutsche Forschungsgemeinschaft (DFG) of Germany. Additionally, this work was supported by the Ministry of Commerce, Industry and Energy (MOCIE).

Supporting Information Available: Figures S1−S7 (PDF). This material is available free of charge via the Internet at http://pubs.acs.org.

CM801421W